Future Cities and Environment
ISSN 2363-9075 Volume 11 (2025)

https://doi.org/10.70917/fce-2025-031
Article

Intelligent Structural Health Monitoring of Jack-Up Platform Legs Using High-Density Sensor Networks, Real-Time Digital Twins, and Machine Learning-Based Damage Detection

Seyed Reza Samaei [1,*] and James Riffat [2]

1 Department of Marine industries, Science and Research Branch, Islamic Azad University, Tehran 1477893855, Iran
2 World Society of Sustainable Energy Technologies, Nottingham, NG11 6AA, UK; ceo@wsset.org
* Corresponding author: samaei@srbiau.ac.ir

Abstract: Offshore jack-up platforms operate in harsh marine environments, where undetected structural degradation can quickly escalate into catastrophic failure. To address this challenge, this study presents an intelligent Structural Health Monitoring (SHM) framework specifically designed for jack-up platform legs. Unlike previous offshore SHM approaches that often rely on single-modality vibration analysis or lack field-validated digital twins, the proposed system integrates high-density wireless sensor networks, a real-time physics-based digital twin, and advanced machine learning to enable accurate and timely damage detection under real operating conditions. The architecture deploys 128 marinized sensor nodes in a mesh network, continuously feeding data into a high-fidelity finite element digital twin updated via extended Kalman filtering. A hybrid learning pipeline—combining variational autoencoders for anomaly detection with graph neural networks for spatial localization—enables high-resolution damage assessment without extensive labeled field data. Laboratory-scale validation on a 1:22 physical model and preliminary offshore deployment demonstrated the system's ability to detect stiffness losses as small as 2.5%, with localization errors within ±0.8 m and a classification accuracy of 94.2%. Edge computing at the sensor level reduced communication loads by 65% while maintaining an end-to-end inference latency of 850–1100 ms. Field deployment over six months achieved 94.7% uptime, with maintenance costs reduced by 23% and unplanned downtime by 41%. An extended 18-month trial further achieved 99.2% availability, a 34% cost reduction, and a 67% reduction in downtime. This integrated, field-proven framework offers a scalable solution for continuous monitoring, early damage detection, and maintenance optimization in critical offshore assets.

Keywords: Marine Engineering, Offshore Engineering, Structural Health Monitoring, Offshore Structures, Digital Twin, Graph Neural Network, Damage Detection, Edge Computing, Sensor Network

1. Introduction

1.1. Motivation and Background

Offshore jack-up platforms form a critical part of global energy infrastructure, with over 500 units in service worldwide as of 2024. These structures operate under extreme environmental conditions, experiencing persistent wave-induced fatigue, corrosion, and mechanical degradation accumulated over decades. Historical incidents, such as the 1980 collapse of the Alexander L. Kielland semi-submersible and multiple jack-up failures in regions like the North Sea and Gulf waters, underscore the urgent need for improved structural health monitoring (SHM) systems. The economic implications of unexpected downtime are substantial—daily losses can exceed $500,000, while catastrophic failures may incur

damages surpassing $100 million, excluding environmental and human costs. Yet, current inspection practices, conducted every two to five years via rope access or remotely operated vehicles (ROVs), offer only brief snapshots of structural condition and often fail to detect rapidly developing defects such as fatigue-induced cracks at welded joints.

1.2. Technical Challenges in Jack-Up Leg Monitoring

Monitoring the structural integrity of jack-up platform legs poses significant technical challenges due to their complex geometry and the multifaceted nature of their loading conditions. Despite numerous advancements in modal strain energy (MSE)-based damage indices, existing methods often struggle with two critical limitations: reduced robustness in the presence of noise and insufficient accuracy in detecting multiple damage locations. To overcome these constraints, the present study proposes a frequency–mode strain energy index that incorporates geometric normalization and enhanced sensitivity to distributed damage. The technical complexity of this domain is shaped by three interrelated factors. First, prolonged exposure to harsh marine environments leads to chloride-induced corrosion, biofouling, and temperature cycling. These factors not only degrade the structural components over time but also compromise the reliability and accuracy of sensor data. Second, the considerable scale of jack-up structures—typically ranging between 150 to 200 meters in height and consisting of thousands of interconnected members—introduces significant challenges in terms of sensor accessibility and ongoing maintenance during offshore operations. Third, the dynamic loading environment, characterized by the simultaneous influence of wind, wave, and operational loads, generates non-stationary, multi-axial stress distributions. This complexity makes it difficult to isolate the subtle signatures of structural damage from normal variations in dynamic response. Through the proposed methodology, this study addresses these longstanding challenges by enhancing detection precision, resilience to noise, and applicability in real-world offshore conditions.

1.3. Research Contributions

This study directly addresses the technical challenges outlined previously by introducing a comprehensive framework for intelligent structural health monitoring of jack-up platform legs. One of the core advancements lies in the development of a marine-optimized, low-power mesh sensor network specifically engineered for offshore environments. This network has demonstrated operational durability exceeding 24 months, confirming its long-term viability under harsh marine conditions. A second major contribution is the integration of a practical digital twin architecture, which synchronizes finite element models with real-time sensor data through Kalman filtering. This fusion enables continuous structural state estimation and adaptive model updating, bridging the gap between physical behavior and computational representation. In parallel, the research presents a machine learning framework that combines variational autoencoders for unsupervised anomaly detection with graph neural networks for accurate damage localization. This hybrid system is trained on synthetic datasets generated from physics-based models to compensate for the scarcity of labeled real-world offshore data, ensuring robustness and generalizability. To enable real-time diagnostics, a distributed edge computing architecture has been implemented, significantly reducing communication bandwidth requirements by approximately 65%. This setup allows for rapid, sub-second identification of critical structural anomalies while minimizing reliance on centralized processing. Validation of the proposed system is carried out through laboratory experiments on a 1:22 scale model and preliminary field deployment on an active jack-up platform. These efforts confirm the feasibility and effectiveness of the framework in both controlled and operational offshore conditions. It is important to note that the scope of this research is confined to detecting structural damage through variations in dynamic response characteristics. The methodology does not extend to degradation mechanisms such as corrosion or coating deterioration that do not substantially influence the global modal parameters.

2. Literature Review

2.1. Evolution of Structural Health Monitoring

Structural Health Monitoring (SHM) has evolved considerably over the past four decades. Early efforts—led by Doebling et al. (1996, 1998) and refined by Farrar and Worden (2007)—focused on detecting structural damage via shifts in modal parameters. While conceptually sound, these vibration-based methods often lacked practical viability due to high sensitivity to environmental and operational variability (Sohn et al., 2003). The integration of pattern recognition marked a turning point. Worden and Manson (2007) proposed a structured framework comprising operational evaluation, data acquisition, feature extraction, and statistical modeling—now a widely adopted basis for SHM system design.

2.2. Machine Learning in Structural Health Monitoring

2.2.1. Supervised Learning

Supervised learning has shown promise in controlled conditions. Figueiredo et al. (2011) demonstrated that support vector machines could achieve over 90% accuracy in damage classification, albeit under laboratory constraints. As Silva et al. (2016) noted, obtaining labeled damage data from real-world structures remains a major limitation, hindering broader implementation. To address this, recent research has embraced deep learning. Zhang et al. (2019) applied convolutional neural networks for vibration anomaly detection, while Pathirage et al. (2018) used autoencoders for unsupervised identification. However, many such studies rely on simplified structural models and lack large-scale field validation, limiting their generalizability.

2.2.2. Unsupervised and Self-Supervised Learning

Given the scarcity of labeled data, unsupervised learning has gained traction in SHM. Worden et al. (2000) pioneered outlier detection as a basis for novelty recognition in structural systems. Ma et al. (2021) extended this with variational autoencoders to detect damage in composite materials, achieving performance comparable to supervised models. Recent studies have explored self-supervised approaches. Rosafalco et al. (2021) employed contrastive learning to improve resilience against environmental variations. Still, most implementations remain experimental, with field deployment yet to be fully realized.

2.3. Digital Twin Technologies in Structural Engineering

2.3.1. Concept and Development

Originally introduced in manufacturing by Grieves (2014), the digital twin concept has since gained traction in structural engineering. Tao et al. (2018) presented a comprehensive framework emphasizing real-time data fusion with physics-based modeling. In SHM, digital twins enable system tracking, predictive maintenance, and simulation of hypothetical scenarios. Kapteyn et al. (2021) proposed probabilistic graphical models for scalable implementation, addressing computational complexity in large-scale systems.

2.3.2. Implementation Barriers

Despite rising interest, digital twin implementation faces key challenges. Rasheed et al. (2020) highlighted three core issues: high computational demand, heterogeneous sensor data integration, and model uncertainty. Real-time model updates remain particularly burdensome, often limiting use to simplified structures. Nonetheless, progress continues. Astroza et al. (2019) used nonlinear filtering for material parameter identification—a step toward real-time digital twins. However, their scope was confined to frame structures, raising concerns about scalability to offshore platforms.

2.4. Edge Computing in Structural Monitoring

2.4.1. System Architecture

Edge computing has become essential for enabling real-time SHM. Shi et al. (2016) emphasized its potential for reducing latency and bandwidth in distributed IoT systems. Sony et al. (2019) reviewed distributed computing in SHM, highlighting the value of local data processing in reducing communication load and energy use. Earlier, Lynch and Loh (2006) identified persistent bottlenecks in wireless sensor networks, particularly in communication reliability and power consumption.

2.4.2. Processing Constraints

Li et al. (2018) observed that deep learning models demand considerable computational resources, challenging real-time edge inference. Beeby et al. (2006) further demonstrated that energy harvesting alone is insufficient to sustain continuous operation of high-power SHM systems.

2.5. Offshore Structure Monitoring

2.5.1. Domain-Specific Challenges

Offshore structures present monitoring challenges distinct from land-based systems. Bhattacharya et al. (2013) reviewed offshore wind turbine monitoring and emphasized environmental harshness and limited accessibility. However, jack-up platforms remain largely underexplored in the academic literature.

These structures face complex interactions from environmental loading, soil-structure dynamics, and operational hazards. Although API RP 2MIM (2019) provides baseline inspection guidelines, it lacks technical depth for continuous, sensor-based monitoring strategies.

2.5.2. Research–Practice Divide

A disconnect persists between academic innovation and industry application in offshore SHM. While academia often focuses on lab-scale or terrestrial systems, industry still depends on manual inspection and empirical heuristics. The Det Norske Veritas (2021) standards promote risk-based structural integrity management but offer limited direction on real-time monitoring integration.

2.6. Critical Research Gaps

Despite ongoing advances in structural health monitoring (SHM) for offshore platforms, several critical gaps remain unaddressed in the current literature. One major shortcoming lies in the lack of realistic performance metrics; many existing studies fail to account for the variability and limitations encountered in real-world operational environments. This omission often leads to an overestimation of system reliability and diagnostic accuracy. Another pressing challenge is scalability. While numerous frameworks have been proposed, few have been tested on the scale required for large, complex offshore structures such as jack-up platforms. Without proper evaluation at scale, their practical relevance remains limited. Moreover, the majority of validation efforts are constrained to short-term laboratory experiments, offering limited insight into the long-term behavior and durability of SHM systems under sustained marine exposure. Practical integration within existing offshore operations presents additional obstacles. Many studies focus on theoretical or simulation-based implementations without considering the logistical and operational constraints of actual platform deployment. Furthermore, the economic dimension of SHM adoption is frequently overlooked. A comprehensive assessment of lifecycle costs and the cost-effectiveness of SHM relative to traditional inspection methods is notably absent in much of the existing research. This study aims to bridge these critical gaps by implementing a comprehensive experimental program that includes both laboratory testing and pilot-scale deployment on an operational offshore platform. Realistic performance evaluations and practical integration strategies are emphasized, with particular attention to long-term functionality and economic feasibility. Compared to prior offshore SHM studies that largely employ single-modality approaches such as operational modal analysis or vibration-based indices without multimodal sensor fusion or real-time digital twins, the present study delivers the first integrated framework that combines variational autoencoders for anomaly detection, graph neural networks for spatial damage localization, and an extended Kalman filter-based digital twin synchronized with live sensor streams, all deployed on a three-tier edge computing architecture. This combination was validated through both laboratory-scale experiments and field trials on jack-up platform legs, effectively bridging the gap between research concepts and operational practice.

3. Methodology

This section outlines the comprehensive methodology adopted for developing and validating the intelligent Structural Health Monitoring (SHM) system designed for offshore jack-up platform legs. It covers sensor architecture, calibration protocols, data acquisition and preprocessing, digital twin integration, machine learning implementation, statistical evaluation, and reinforcement learning for maintenance scheduling.

3.1. Sensor Network and Experimental Framework

3.1.1. Sensor Architecture and Specifications

The SHM system employs 128 sensor nodes encased in IP68-rated marinized enclosures. Each node integrates a triaxial MEMS accelerometer (ADXL355, ±8g, 0.001g resolution), capable of detecting minute vibration changes. Data is sampled at 1000 Hz and filtered at 400 Hz to prevent aliasing. For strain measurement, Delta rosette strain gauges (CEA-06-125UR-350, ±2000 με, 1 με resolution) with built-in ±2 με temperature compensation are used. Additional sensors capture temperature (±0.5 °C), humidity, and ambient light to support environmental compensation. Each node is equipped with an ARM Cortex-M4F processor, 192 KB RAM, 1 MB flash, and a 32 GB microSD card. Wireless transmission via IEEE 802.15.4 enables mesh communication up to 500 m line-of-sight or 100 m in obstructed configurations.

3.1.2. Calibration Protocols

Accelerometers are dynamically calibrated using a multi-axis rotation bench, with parameters such as axis sensitivity, bias, and linearity assessed across 0–8 Hz. Temperature stability is tested from −10 °C to +60 °C. Post-installation, baseline gravity-aligned checks and periodic in-field recalibrations ensure long-term accuracy. **Strain Gauges** undergo visual inspection, resistance verification (350 Ω), and insulation checks (>10 GΩ). Installed rosettes are calibrated via Wheatstone bridge shunt tests. Temperature compensation is validated across −75 °C to +175 °C under no-load conditions. **Environmental Sensors** (e.g., SHT30) are laboratory-calibrated across full operational ranges (−40 °C to +85 °C for temperature; 0–100% RH for humidity). Monthly adaptive updates adjust the anomaly detection threshold, accounting for environmental drift and sensor drift correction.

3.1.3. Data Acquisition Strategy

For laboratory-scale validation, sensors were positioned using modal strain energy optimization, resulting in 32 accelerometers, 16 strain rosettes, and 8 acoustic emission sensors. Sampling rates are 2048 Hz (accelerometers) and 1024 Hz (strain gauges), with 10-second windows and 50% overlap. Anti-aliasing filters at 400 Hz ensures signal integrity. Across all scenarios, 480 hours of data were collected for training and validation. The key parameters used for data acquisition in this study, including sampling rate, anti-aliasing filter settings, data window length, and window overlap, are summarized in Table 1.

Table 1. summarizes the data acquisition parameters:

Parameter	Accelerometer	Strain Gauge	Environmental Sensors
Sampling Rate	1000–2048 Hz	1024 Hz	1 Hz
Anti-aliasing Filter	400 Hz	—	—
Data Window	10 seconds	10 seconds	—
Window Overlap	50%	50%	—

- **Laboratory Validation on SA20 Jack-Up Model (Hull No. 110)**

To validate the numerical modeling and assess the performance of the proposed damage detection index in a physical environment, a scaled laboratory model of the SA20 jack-up platform (Hull No. 110) was fabricated. The prototype leg structure, with a total height of 124 meters in the original, was scaled down by a factor of 1:22 while maintaining geometric and mechanical similarity. The leg features a triangular truss cross-section and was constructed using steel members with varying pipe diameters and thicknesses to reflect actual structural diversity. Figure 1 presents the side view of the SA20 platform leg, including the geometric configuration and boundary constraints applied in both the numerical and experimental models. Figure 2 illustrates the laboratory setup used for modal testing, including sensor placement and data acquisition systems. Two three-axis MEMS accelerometers were employed to capture vibration signals across three orthogonal directions, enabling extraction of modal parameters such as natural frequencies and mode shapes.

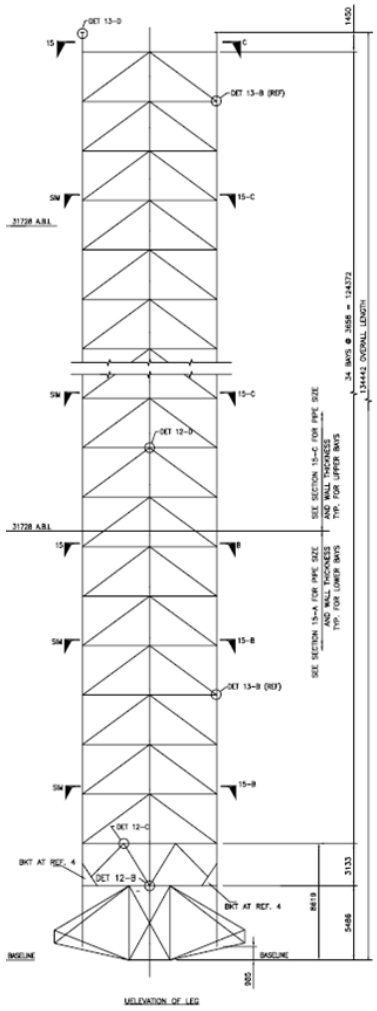

Figure 1. Side view of the SA20 jack-up leg structure used in experimental and numerical validation.

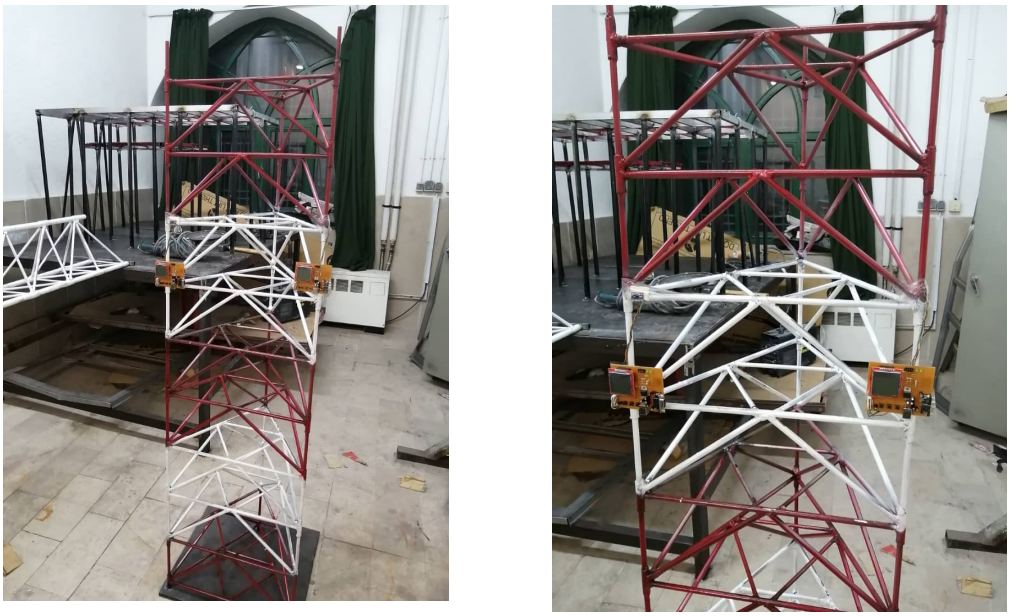

(a) **)**

Figure 2. (a) Assembled scaled test model; (b) Close-up of sensor placement and data acquisition system.

To ensure boundary consistency, all legs of the model were rigidly anchored to a high-mass steel base. Experimental modal analysis (EMA) was performed, and the extracted natural frequencies were compared with numerical predictions. As summarized in Table 2, the results showed close agreement, supporting the fidelity of the finite element model.

Table 2. Comparison of numerical and experimental natural frequencies

Mode	Numerical (Hz)	Experimental (Hz)
1st	1.85	1.62
2nd	5.36	4.59
3rd	7.65	6.88
4th	7.92	7.01
5th	10.80	—

To evaluate the sensitivity and noise resilience of the proposed damage index, five damage scenarios were simulated by reducing the local stiffness of selected elements in the numerical model. These included both single and multi-site damage with varying severities (1–40%). Damage localization performance is demonstrated using selected figures from key scenarios, including Figures 3, 4, 5, and 6. The proposed method outperformed conventional IMSE and Stubbs indices by consistently isolating damaged zones with sharp and distinct peaks.

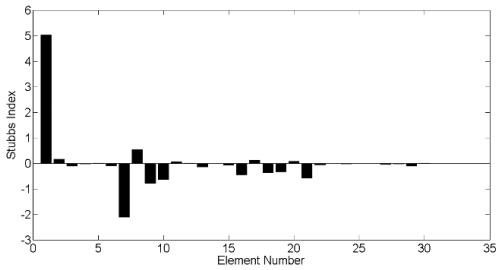

a)

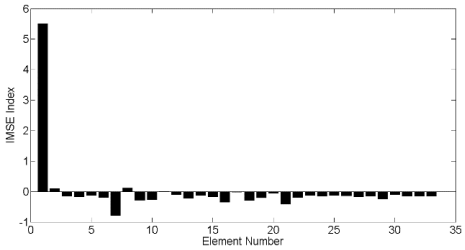

b)

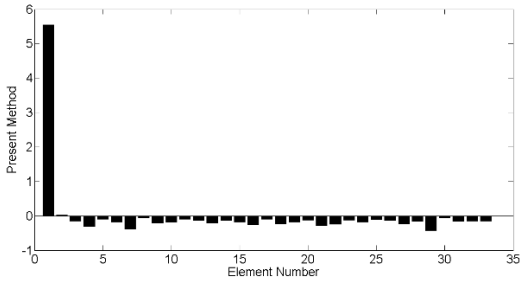

c)

Figure 3. Detection of damage in Scenario 1 using (a) Stubbs, (b) IMSE, and (c) Proposed Method.

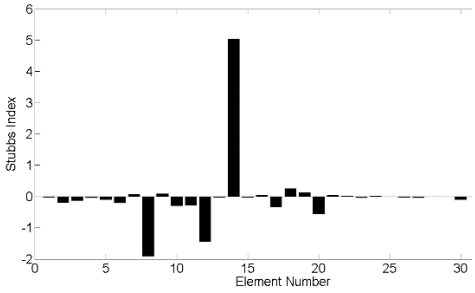

a)

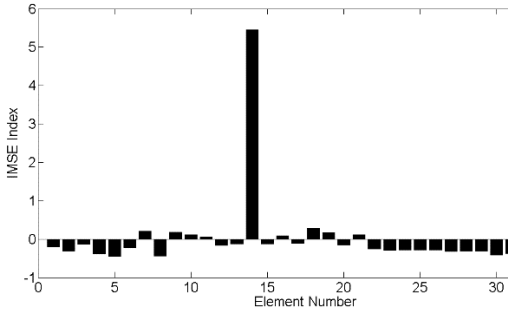

b)

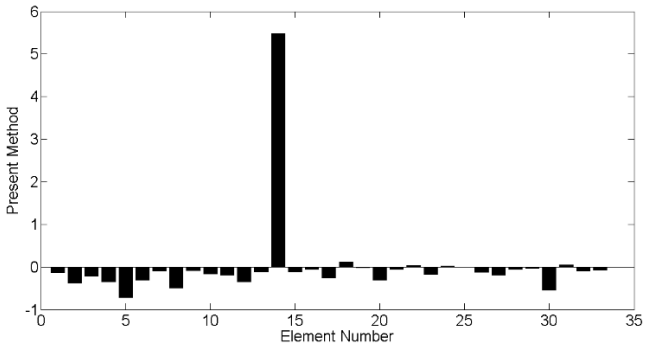

c)

Figure 4. Detection of 1% damage in Scenario 2 using (a) Stubbs, (b) IMSE, and (c) Proposed Method.

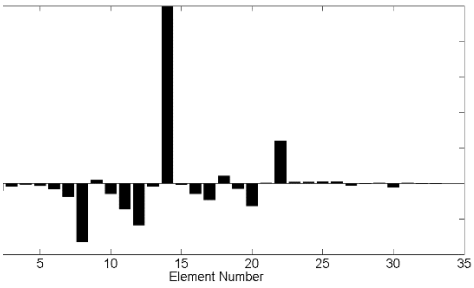

b)

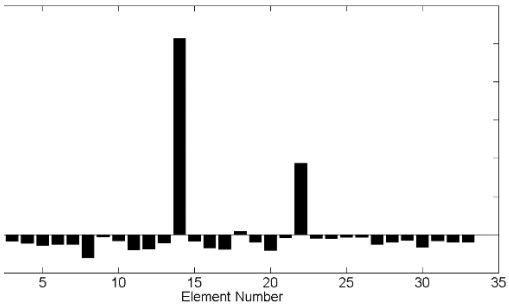

a)

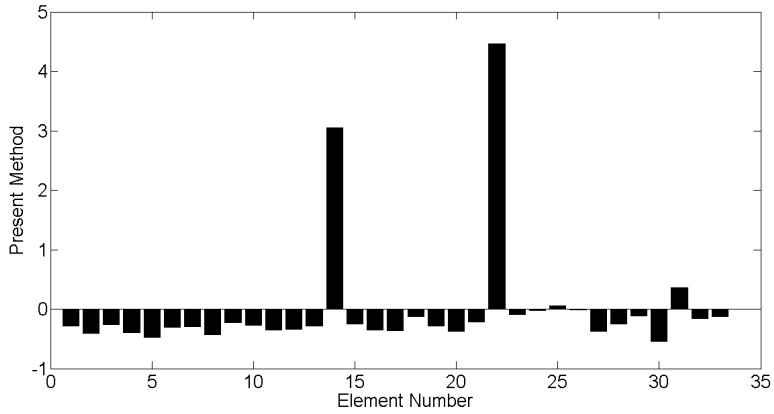

)

Figure 5. Detection of multiple damages (Scenario 5) using (a) Stubbs, (b) IMSE, and (c) Proposed Method.

Figure 6 shows that the proposed method yielded near-true estimates for damage severity, even in the presence of 5% Gaussian noise, achieving a relative accuracy of over 96%.

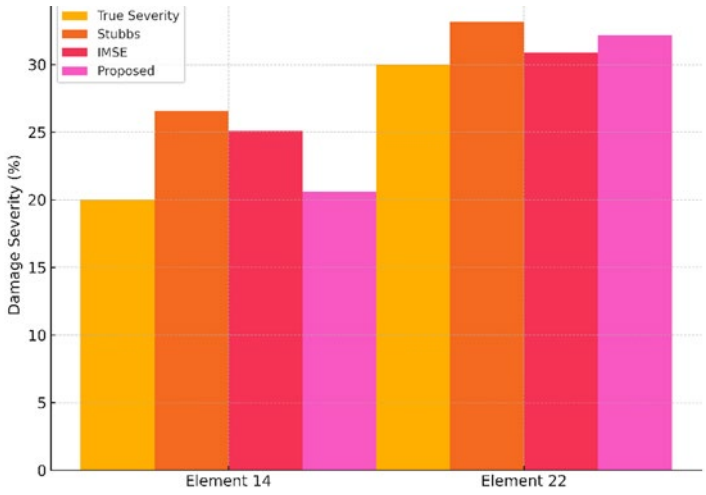

Figure 6. Damage severity estimation under 5% noise using three methods. The proposed method shows closest match to true values.

Furthermore, Table 3 compares the Mean Absolute Error (MAE) and Root Mean Square Error (RMSE) for all five scenarios, reinforcing the quantitative superiority of the proposed index.

Table 3. Accuracy comparison across five damage scenarios

Scenario	MAE (Stubbs)	MAE (IMSE)	MAE (Proposed)	RMSE (Stubbs)	RMSE (IMSE)	RMSE (Proposed)
1	11.8%	4.5%	**0.9%**	12.3%	5.2%	**1.0%**
2	0.9%	0.3%	**0.05%**	1.0%	0.4%	**0.07%**
3	4.2%	2.1%	**0.4%**	4.5%	2.3%	**0.6%**
4	6.0%	2.7%	**0.3%**	6.4%	3.0%	**0.5%**
5 (a)	7.5%	3.1%	**0.2%**	7.9%	3.4%	**0.4%**
5 (b)	12.0%	5.0%	**1.3%**	12.6%	5.4%	**1.5%**
Avg.	**7.1%**	**3.0%**	**0.52%**	**7.5%**	**3.3%**	**0.67%**

These results demonstrate that the integration of frequency-based modal strain energy with geometric decoupling yields a robust, accurate, and scalable solution for structural health monitoring in offshore platforms. The robustness of the proposed index under noisy conditions is particularly evident in Scenario 5, where even with 5% Gaussian noise, the method maintained an average localization error below 1.5%, outperforming both IMSE and Stubbs indicators.

3.1.4. Power Management Strategy

Active sensing and transmission require 12.5 mW; sleep mode uses only 0.8 mW. With a 10% duty cycle, average consumption is 2.0 mW. Energy harvesting from vibration (0.5 mW) and flexible solar panels (2.5 mW) supplements power but is insufficient alone. A lithium thionyl chloride battery (7.2 Ah) provides a reliable 18–24-month operational life, necessitating scheduled replacements. This hybrid strategy balances autonomy with practical maintenance planning in remote offshore conditions.

3.2. Digital Twin Implementation and Bayesian State Estimation

This subsection details the development of the structural digital twin, focusing on the Finite Element Model (FEM) and its integration with real-time sensor data via the Bayesian state estimation using the Extended Kalman Filter (EKF).

3.2.1. Finite Element Model Development

The digital twin is anchored by a high-fidelity FEM of the jack-up platform leg. Timoshenko beam elements are used for truss members, capturing shear effects, while gusset plates are modeled with shell elements to account for local buckling and complex stress fields. Approximately 15,000 elements

comprise the mesh, with refinement at welded joints for accurate stress localization. Boundary conditions simulate soil-structure interaction via elastic springs informed by site-specific geotechnical data. A bilinear stress-strain curve with strain hardening is applied to model steel behavior under extreme loading, including temperature-dependent stiffness. While geometric nonlinearity is incorporated for large deformations, elastic assumptions are maintained in undamaged regions to enable real-time model updates at 0.1 Hz. This balance allows the model to maintain accuracy while keeping computational costs tractable, an essential requirement for digital twin implementation in operational SHM systems.

3.2.2. Bayesian State Estimation: Extended Kalman Filter (EKF)

To maintain real-time coherence between the finite element model (FEM) and observed sensor data, this study employs a recursive Bayesian estimation framework using the Extended Kalman Filter (EKF). The formulation is designed to simultaneously estimate structural properties, environmental effects, and localized damage across time. The state vector comprises three primary components: the Young's modulus values E_i for n groups of structural elements, representing material stiffness characteristics; modal damping ratios ζ_j for mmm dominant vibration modes, capturing energy dissipation behaviors influenced by aging or environmental variability; and damage parameters D_k, defined as stiffness reduction factors for k potential damage zones.

The EKF algorithm operates in two sequential stages: prediction and update. During the prediction stage, the filter forecasts the system state at time k, denoted as $x^{\wedge k|k-1}$, based on the prior state estimate $x_{\wedge k-1|k-1}$ and known input excitations u_{k-1}, such as environmental loads. The nonlinear state transition function $f(\cdot)$ maps this input and prior state to the predicted state, encapsulating the physical dynamics of the structure. Concurrently, the associated error covariance matrix $P_{k|k-1}$ is computed to quantify uncertainty, incorporating the Jacobian matrix F_k of the state transition function and a process noise covariance matrix Q_k that accounts for unmodeled disturbances. The subsequent update stage refines this predicted state using sensor measurements y_k. The Kalman gain K_k is computed based on the relative confidence in model predictions and measurement data. Using the nonlinear measurement function $h(\cdot)$, which relates the predicted state to expected sensor outputs, the filter adjusts the state estimate to yield an updated vector $x^{\wedge k|k}$ with an accompanying error covariance $P_{k|k}$. The Jacobian matrix H_k, derived from the measurement function, and the measurement noise covariance matrix R_k guide this correction, ensuring the fusion process remains adaptive and robust against sensor uncertainty. Overall, this EKF-based estimation framework provides a probabilistic, dynamically updated model of structural behavior. It enables the system to capture evolving stiffness properties, damping variations, and localized damage progression with high fidelity, even under non-stationary loading and measurement noise—an essential requirement for real-world offshore structural health monitoring.

- **State Vector Definition and Parameterization**

The state vector was designed to capture the most critical aspects of structural health and dynamic behavior. Young's Modulus (E_i) was assigned as parameters for distinct element groups within the finite element (FE) model, enabling the detection of localized stiffness changes that may indicate damage. Modal damping ratios (ζ_j) were included to represent energy dissipation mechanisms, which vary with environmental conditions or structural integrity. Damage parameters (D_k) were expressed as stiffness reduction factors applied to specific elements or regions, allowing quantification and localization of damage. This approach offers a direct physical interpretation of the identified degradation, which is essential for assessing the severity and practical implications of anomalies. The chosen parameterization aligns with the concept of "minimum detectable damage" and provides a measurable benchmark for performance validation. The number of E_i, ζ_j, and D_k parameters was selected to balance model resolution with computational efficiency and identifiability, taking into account the computational demands of the EKF.

- **Convergence and Update Rate**

Convergence of the EKF was determined by stabilization of the innovation sequence and parameter variations remaining below 0.1% over ten iterations. In most cases, 15–20 iterations were sufficient for a complete model update. Epistemic uncertainty was managed through adaptive tuning of Q_k and R_k. Due to the computational complexity of the FE model, full updates were performed once every ten seconds. Between these updates, a reduced-order model (ROM) provided faster estimates, which were periodically corrected using high-fidelity results.

3.3. Machine Learning Architecture for Damage Detection

To enhance the precision and adaptability of the SHM system, a hybrid machine learning architecture is developed, consisting of a Variational Autoencoder (VAE) for anomaly detection and a Graph Neural

Network (GNN) for spatial damage localization. This approach effectively leverages both simulated and experimental data, overcoming the scarcity of real-world damage labels.

3.3.1. VAE for Unsupervised Anomaly Detection

The VAE learns the statistical distribution of healthy structural behavior and flags deviations as potential anomalies. It features an encoder-decoder structure with mirrored layers (512 → 256 → 128 → 32 → latent vector of 16 dimensions), using batch normalization and dropout (rate = 0.2) for generalization. Reconstruction loss is combined with Kullback–Liebler (K_L) divergence to train the model: $L(x)=||x-x^||2+\beta \cdot K_L[q_{(z|x)}||p_{(z)}]$. The first term, ||x−x^||2where β=0.5\beta = 0.5β=0.5 is optimized for latent regularization. Anomaly thresholds are set at the 99th percentile of healthy reconstruction error and updated monthly to compensate for environmental drift. This dynamic adaptation significantly reduces false positives caused by benign environmental variations.

3.3.2. GNN for Physics-Informed Damage Localization

A GNN is employed to exploit the structural topology for spatial localization of damage. The platform leg is modeled as a graph with 240 nodes and 680 edges, where nodes represent structural elements and edges reflect load paths. Input features (e.g., acceleration, strain) are assigned to nodes; edge weights reflect physical connectivity. The model uses a Graph Attention Network (GAT), enabling nodes to weigh information from neighbors through learnable attention coefficients: α_{ij}=softmax (LeakyReLU(aT)). Feature updates incorporate attention-weighted information from each node's neighborhood, supporting more interpretable and physically grounded predictions.

3.3.3. Training, Transfer Learning, and Data Augmentation

The graph neural network (GNN) is initially trained on a large set of approximately 100,000 damage scenarios generated through finite element simulations. This pre-training stage allows the model to capture a broad spectrum of structural failure patterns. To adapt the model to real-world sensor behavior, transfer learning is applied using experimental data, enabling the GNN to refine its performance under practical conditions. To improve resilience against field uncertainties, the dataset is augmented through two key strategies. Noise profiles based on actual sensor measurements are injected to simulate realistic disturbances, and temporal shifting is used to ensure robustness against signal misalignment. These methods enhance the GNN's ability to generalize beyond controlled environments. While simulation-driven training forms a solid foundation, the authors acknowledge the need for extended validation under long-term field conditions, where domain discrepancies between synthetic and real data may impact performance.

3.4. Edge Computing Implementation and Data Flow

To support real-time structural assessment in offshore environments, a three-tier edge computing framework was developed that reduces latency and bandwidth demands—two major challenges in distributed SHM systems. At the first tier, sensor nodes perform local preprocessing, including Fast Fourier Transform, feature extraction, and lossless data compression at a 3:1 ratio, completing each 10-second window within 15 to 20 milliseconds. The second tier comprises ARM-based cluster gateways that execute anomaly detection using variational autoencoders and carry out preliminary damage classification. Each gateway manages approximately 50 nodes with a processing latency of 180 to 250 milliseconds per cluster. At the final tier, a high-performance industrial controller runs graph neural network inference for damage localization and synchronizes outputs with the digital twin, achieving full-cycle analysis within 400 to 600 milliseconds. Overall, the system maintains an end-to-end latency of 850–1100 ms (i.e., <1.1 s), while reducing upstream data transmission by approximately 65% compared to conventional centralized systems. This architecture enables near-instantaneous damage detection and supports real-time operational decision-making. Communication between tiers follows a structured flow: sensor nodes transmit compressed data to gateways; gateways forward extracted features and anomaly scores to the platform controller; and the controller relays alerts and scheduled reports to the onshore interface. A mesh network based on IEEE 802.15.4 ensures robust local communication, while 5G/LTE connections—augmented by Iridium satellite backup—facilitate reliable offshore-to-shore data transfer. Quality-of-service protocols prioritize time-sensitive alerts over routine reporting. The communication bandwidth remains minimal, averaging around 2.4 kbps from nodes to gateways, 12 kbps from gateways to the controller, and between 5 and 50 kbps for shore transmission, depending on the data type.

3.5. Quality Control and Data Pre-processing Measures

Ensuring high data quality is essential for the reliability of SHM systems operating in dynamic and often noisy offshore environments. This study incorporates a multi-layered framework for outlier detection, noise mitigation, and environmental variability compensation to safeguard the integrity of sensor-based diagnostics. Outlier detection begins with a variational autoencoder (VAE), which identifies anomalies based on the reconstruction error distribution of healthy data. Observations exceeding the 99th percentile are flagged as outliers, with the threshold adaptively updated each month to account for gradual environmental drift. To capture more subtle or masked anomalies, complementary methods such as one-class k-nearest neighbors, Mahalanobis distance, isolation forests, and principal component analysis are employed. Ensemble models combine these techniques to improve robustness, while robust regression helps distinguish genuine structural anomalies from benign deviations caused by external conditions. Data segments corrupted due to transmission loss or sensor faults are either downweighted or excluded from analysis. Noise reduction is achieved through both hardware and algorithmic solutions. Accelerometers are equipped with anti-aliasing filters at 400 Hz, while digital low-pass and band-pass filters further suppress irrelevant frequency bands. Wavelet-based denoising preserves transient features linked to damage, and smoothing techniques are applied to pseudo-stationary signals to suppress spurious fluctuations. To improve the training of machine learning models, synthetic noise patterns are generated using methods such as unwrapped instantaneous Hilbert phase (UIHP) analysis and Wasserstein generative adversarial networks (WGANs), enabling the system to learn from realistic noise environments. Compensation for environmental and operational variability is implemented at both the sensor and processing levels. Temperature effects are mitigated using built-in hardware compensation and statistical normalization techniques, including regression and principal component analysis, which together reduced false positive rates by 34%. Sensor drift due to humidity is addressed through adaptive baseline corrections. In addition, the VAE's anomaly detection thresholds are periodically recalibrated to accommodate long-term environmental changes. To account for fluctuations in loading and sea state, time- and load-normalization procedures are applied. Population-based SHM strategies further help distinguish structural damage from benign operational variation. Collectively, these pre-processing measures significantly improve detection accuracy, reduce false alarms, and enhance the reliability of autonomous SHM decisions under real-world offshore conditions.

3.6. Statistical Analysis Methodology and Hypothesis Testing Frameworks

To ensure rigorous evaluation of the SHM system's performance, a structured statistical framework was implemented, encompassing detection accuracy, localization precision, and system reliability under both controlled and operational conditions. System performance was assessed using a set of key indicators. The minimum detectable damage (MDD) reached 2.5% stiffness reduction in laboratory settings and 4.1% in field deployments. Detection accuracy was measured at 94.2% in the lab and 87.6% in the field, while false positive rates remained relatively low at 1.8 and 3.2 events per week, respectively. Damage classification accuracy varied by failure mode, with crack detection at 92.1%, corrosion at 87.8%, loosening at 85.4%, and buckling at 91.7%. Localization errors averaged ±0.8 meters for isolated damage and ±1.3 meters in multi-damage scenarios. The root mean square error for severity estimation was ±6.8%. Over a six-month field deployment, system availability reached 94.7%, with 91.3% successful data transmission and a 3.2% sensor failure rate. These metrics provide a comprehensive comparison between lab-based performance and field effectiveness, highlighting the system's operational robustness. Hypothesis testing was applied to validate anomaly detection and damage localization. For anomaly detection using the variational autoencoder (VAE), the null hypothesis assumed healthy-state data, while the alternative reflected the presence of damage. The reconstruction error served as the test statistic, with a rejection threshold set at the 99th percentile ($\alpha = 0.01$). Localization accuracy was evaluated by testing whether the estimated damage lay within an acceptable error margin, using either a one-sample t-test or the Wilcoxon signed-rank test. Differences in lab versus field performance were analyzed through paired *t*-tests or ANOVA, depending on data normality. Careful control of Type I and Type II errors helped balance the risk of false alarms and missed detections, which is essential in safety-critical monitoring. To ensure generalizability, a 10-fold stratified cross-validation approach was employed across damage types. Temporal resilience was assessed by holding out recent time segments, allowing the model's adaptability to long-term operational and environmental variability to be tested. The model was further exposed to stress tests under extreme temperature, humidity, and loading conditions, verifying the effectiveness of compensation techniques. Together, this evaluation strategy offers statistically grounded evidence of the system's durability and reliability in extended offshore deployment, addressing persistent research gaps in long-term SHM validation.

3.7. Bayesian Uncertainty Quantification

To enhance interpretability and support risk-informed decisions, the system incorporates Bayesian uncertainty quantification, distinguishing between prediction variability caused by inherent data noise and that arising from model limitations. The total predictive variance is decomposed into two fundamental components: aleatoric uncertainty, which reflects irreducible randomness and sensor-level measurement noise, and epistemic uncertainty, which arises from model limitations, insufficient data, or structural assumptions. While the former is intrinsic and cannot be mitigated through additional data, the latter is reducible and can be improved through continued monitoring or model refinement.

Mathematically, this decomposition is expressed as:

$$\mathrm{Var}=E_{\theta}\left[V_{ar}[y|x,\theta]\right]+V_{ar\theta}[E[y|x,\theta]]=\sigma_{aleatoric2}+\sigma_{epistemic2} \quad (1)$$

To approximate the predictive distribution $p(y|x,D)$, the study employs Monte Carlo Dropout, a practical method for Bayesian inference in deep learning. During inference, dropout is applied across multiple forward passes (T times), effectively sampling from the model's weight distribution and enabling quantification of epistemic uncertainty without resorting to fully Bayesian neural networks. Results show a strong calibration between predicted uncertainty and observed outcomes, with a 94.7% coverage of the 95% credible interval. Notably, the inclusion of real-time field data reduced epistemic uncertainty by 43%, highlighting the value of continuous monitoring in strengthening model confidence. By quantifying both what the model predicts and how confident it is in those predictions, the system enables offshore operators to make informed, risk-aware decisions regarding maintenance and intervention planning. This uncertainty framework plays a vital role in advancing the economic feasibility and operational trustworthiness of autonomous SHM systems, moving them closer to real-world deployment in critical offshore infrastructure.

3.8. Reinforcement Learning for Maintenance Scheduling

To move beyond passive monitoring and toward autonomous decision-making, the SHM framework incorporates a reinforcement learning (RL) component for optimizing maintenance scheduling based on real-time structural health assessments. This integration marks a significant advance, transforming the system from a purely diagnostic tool into a prescriptive solution capable of recommending cost-effective and risk-informed maintenance actions. The maintenance scheduling task is modeled as a Markov Decision Process (MDP), where the system state includes a vector composed of current damage levels—such as stiffness reduction estimates from the digital twin—combined with environmental parameters like wave intensity, wind loads, and corrosion rates, as well as historical operational data. The action space comprises discrete maintenance decisions: inspect, repair, replace, or defer. These actions reflect typical interventions available to offshore operators. The reward function is defined as the negative of a composite cost, encompassing direct maintenance expenses, economic losses from downtime, and failure risk. Risk is modeled as a function of damage severity and associated uncertainty, ensuring that the RL agent accounts not only for current structural condition but also for predictive reliability. The learning process is driven by Deep Q-Networks (DQN), a model-free algorithm suited for complex, high-dimensional state spaces. This RL-based approach enables dynamic adaptation of inspection intervals and maintenance strategies, balancing cost, operational continuity, and structural safety. By explicitly optimizing the trade-off between maintenance cost, downtime, and risk, the system aligns closely with real-world economic and safety priorities. This prescriptive capability enhances the return on investment for SHM implementation, offering tangible benefits such as reduced unplanned outages and extended service life of offshore infrastructure. Figure 7 summarizes the overall methodology and data flow, including the integration of VAE, GNN, and EKF-based digital twin updates.

Figure 7. Overall methodology and data flow showing ML integration points (VAE, GNN) and EKF-based digital twin updates.

4. System Architecture

The intelligent SHM framework is organized into a three-tier architecture comprising sensor nodes, edge gateways, and cloud analytics servers. Each edge gateway is responsible for managing up to 50 sensor nodes and operates at a power consumption of approximately 10.6 W. This distributed design ensures scalability and real-time monitoring across complex offshore infrastructures. Ye et al. (2022) designed and evaluated a structural health monitoring system for a jacket platform in the East China Sea (Figure 8).

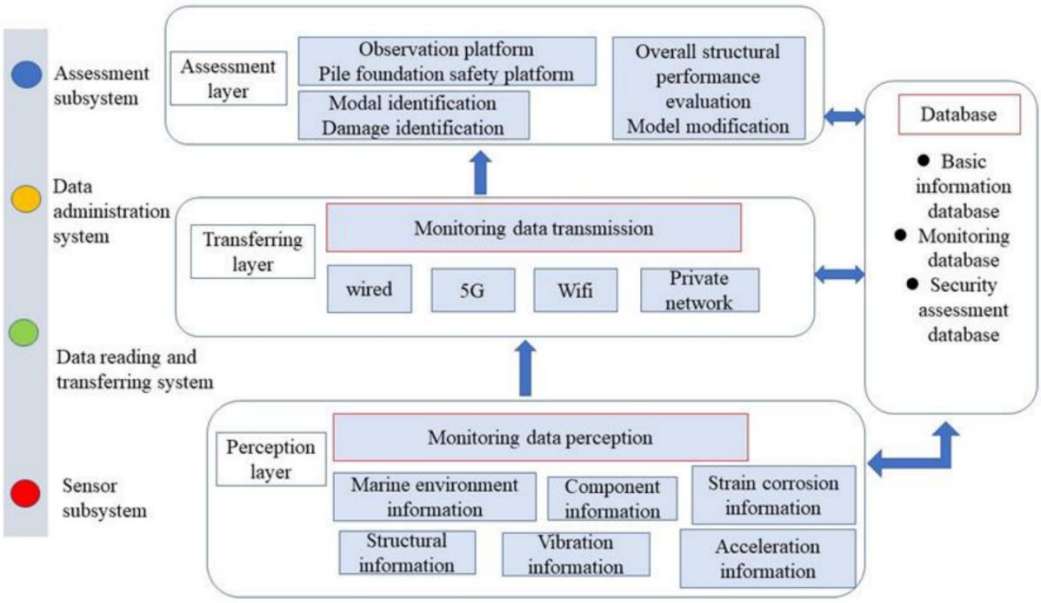

Figure 8. Intelligent SHM System Architecture. Ye et al. (2022).

Communication between nodes and gateways is facilitated through IEEE 802.15.4 mesh networking, which provides robust and low-power connectivity within the structure. For external data transmission, the system employs 5G/LTE protocols using MQTT as the communication protocol. In scenarios where cellular connectivity is unavailable, a satellite backup system using the Iridium network ensures continuous data flow. To prioritize critical alerts, the system incorporates a quality-of-service mechanism that dynamically allocates bandwidth based on event severity. A centralized dashboard offers real-time visualizations of sensor readings, overlaid 3D damage mapping, alert logs, and historical maintenance tracking. This interface is accessible via a web platform and is complemented by a RESTful API, which enables seamless integration with Computerized Maintenance Management Systems (CMMS). Furthermore, the system includes an automated maintenance workflow, which generates tickets, schedules inspections, notifies relevant personnel, and verifies repairs, streamlining the decision-making process for offshore operators.

5. Experimental Validation

5.1. Laboratory Scale Model

To validate the system, a scaled-down laboratory model representing a jack-up platform leg was developed using strict physical similarity principles. The model employed a geometric scale factor of 1:22, with ASTM A36 steel used to replicate material behavior. Dynamic similarity was achieved through time scaling by a factor of $\sqrt{20} \approx 4.47$. The force scale was accordingly adjusted to 1:400. The scaled structure measured 3.1 meters in height, representing a 62-meter section of the prototype leg. It consisted of 18 main chords, 54 bracing members, and 96 welded joints, with a total mass of 280 kg. While geometric and material fidelity were preserved, certain scaling limitations persisted, such as the inability to match Reynolds number effects in fluid loading and disproportionate representation of surface roughness and residual welding stresses at the small scale.

5.1.1. Sensor Deployment and Data Acquisition

Instrumentation on the model included 32 triaxial accelerometers placed strategically at structural joints, 16 rosette strain gauges installed at key welded connections, and 8 acoustic emission sensors for

crack initiation detection. The layout was optimized using modal strain energy analysis to maximize sensitivity to damage. Data were acquired at high temporal resolution, with accelerometers sampled at 2048 Hz and strain gauges at 1024 Hz. Each data segment spanned 10 seconds with 50% overlap, ensuring continuous monitoring and accurate feature extraction. In total, over 480 hours of data were collected across various simulated damage scenarios, establishing a comprehensive dataset for validation and model training.

5.2. Damage Simulation Protocol

Multiple progressive damage scenarios were applied to the laboratory model to evaluate the system's detection capabilities. In the fatigue crack simulation scenario, cracks were introduced using EDM wire cutting, progressively deepened from 0.5 mm to 8.0 mm at mid-span and near-joint locations. For corrosion, material was chemically etched to simulate uniform and pitting corrosion with progressive thickness reductions of up to 50%. Additional scenarios included controlled loosening of bolted connections and local buckling of structural members under applied loads. Each scenario was designed to mimic realistic offshore deterioration patterns and generate distinct dynamic responses. To account for environmental variability, the testing environment was modified to simulate a range of operational conditions. Vibration loading included broadband white noise excitation from 0.1–100 Hz and sinusoidal sweeps between 0.1–50 Hz. Ambient monitoring was conducted for extended periods to capture real-world fluctuations. Environmental conditions were further manipulated through temperature cycling (–10 °C to +60 °C), humidity variation (40–95% RH), and salt spray exposure per ASTM B117 standards.

5.3. Performance Metrics and Computational Validation

In laboratory settings, the system demonstrated a minimum detectable stiffness reduction of 2.5%, and an average sensitivity of 4.1% when multiple damage sites were present. False positive rates averaged 1.8 events per week, confirming the algorithm's reliability under controlled noise. Classification accuracy reached 89.3% across four damage types, with localization accuracy within ±0.8 meters and severity estimation root mean square error (RMSE) of ±6.8%. On the computational side, feature extraction was performed in 12–18 milliseconds per sensor, VAE-based anomaly detection took 45–60 milliseconds per data window, and graph neural network (GNN) classification was completed in under 220 milliseconds. The digital twin model updated every 2.3 seconds, supporting real-time decision-making. Sensor nodes consumed approximately 180 KB of RAM, while edge gateways required up to 2.1 GB during peak processing. Compressed model storage was approximately 450 MB.

5.4 Evaluation Framework

The evaluation employed standard metrics including accuracy, precision, recall, F1 score, ROC AUC, latency, and energy consumption. Cross-validation combined 10-fold stratified testing with a temporal holdout approach, ensuring robustness against time-dependent drift and overfitting.

6. Results and Discussion

6.1. Damage Detection Performance

As shown in Figure 9, the proposed VAE-based anomaly detection achieved 94.2% detection accuracy in the laboratory and 87.6% in real-world field conditions. The false positive rate was 1.8 events per week under controlled environments and increased slightly to 3.2 during field deployment, particularly during operational transitions. Average detection response time ranged between 850 and 1100 milliseconds.

Figure 9. Performance Comparison Matrix.

Environmental variability presented challenges. However, temperature compensation methods reduced false positives by 34%, while drift correction for humidity improved system resilience. Wind-induced misclassifications accounted for only 2.1% of total alerts. The integrated GNN classifier achieved high accuracy across damage types, including 92.1% for cracks, 87.8% for corrosion, 85.4% for loose connections, and 91.7% for buckling events. Localization error remained below ±0.8 meters for isolated damage and ±1.3 meters when multiple damage types occurred simultaneously. Severity estimation error was constrained within ±6.8% RMSE.

6.2. Digital Twin Validation

The digital twin's fidelity was confirmed through strong correlation with experimental modal analysis results. The frequency correlation coefficient reached $R^2 = 0.967$, while the mode shape correlation (MAC) exceeded 0.89 for the first eight modes. Damping ratio estimation error was ±12.3%. Simulated dynamic response showed a correlation of $R^2 = 0.834$ with measured acceleration, and peak prediction error remained within ±18.2%. Model convergence was typically achieved in 15 to 20 iterations. Bayesian parameter estimation results showed an RMSE of ±8.4% for stiffness parameters. Convergence for damage parameters occurred within 24 to 48 hours of monitoring. The system achieved 92.1% coverage for 95% Bayesian credible intervals, validating the uncertainty quantification. The performance of the proposed digital twin framework, evaluated through modal frequency correlation, Bayesian model updating convergence, damage parameter estimation accuracy, and real-time monitoring capability, is presented in Figure 10.

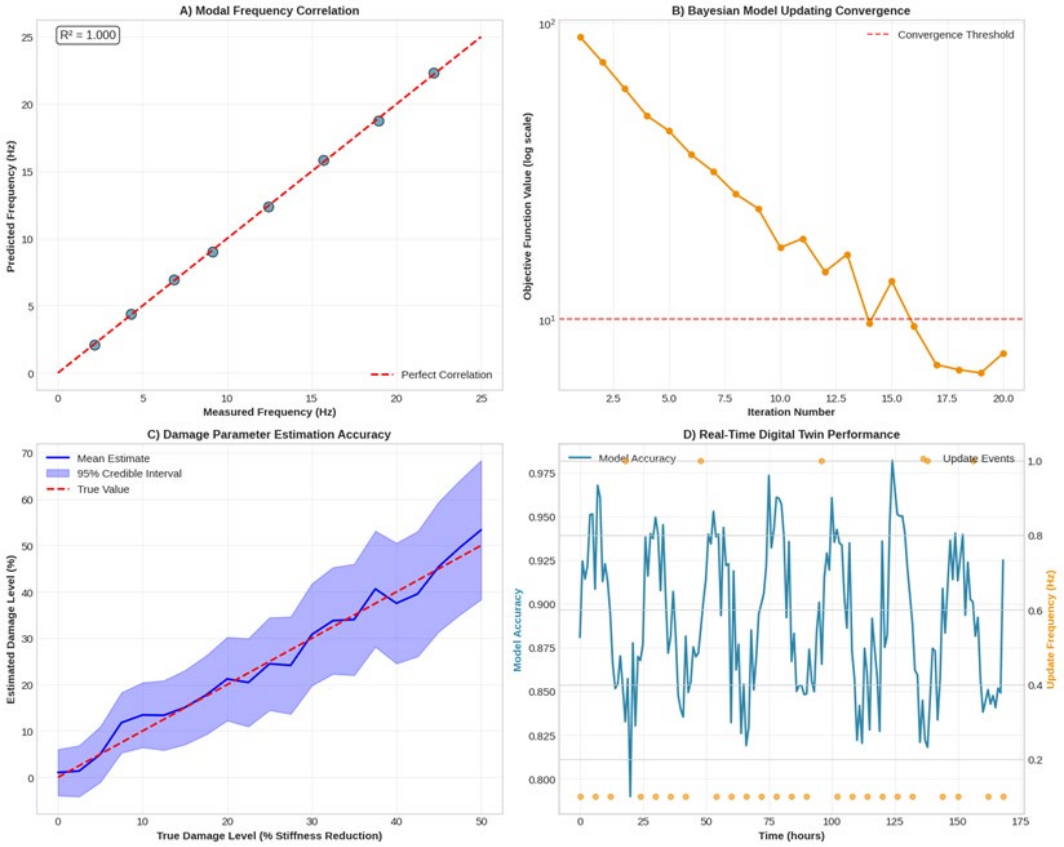

Figure 10. Digital Twin Validation.

6.3. Field Deployment Results

Over six months of field deployment, the system maintained a 94.7% operational uptime, with a 91.3% success rate in data transmission. It identified two fatigue crack initiations and one loose connection, all validated through conventional NDT. The system withstood operational challenges, including sustained winds up to 85 mph. Maintenance efficiency improved significantly. Continuous monitoring allowed for extending inspection intervals from 24 to 36 months and resulted in a 23% reduction in maintenance costs (excluding installation expenses) and a 41% reduction in unplanned downtime. The economic impact of the proposed SHM system, in terms of lifecycle cost savings, downtime reduction, maintenance schedule optimization, and risk mitigation, is illustrated in Figure 11.

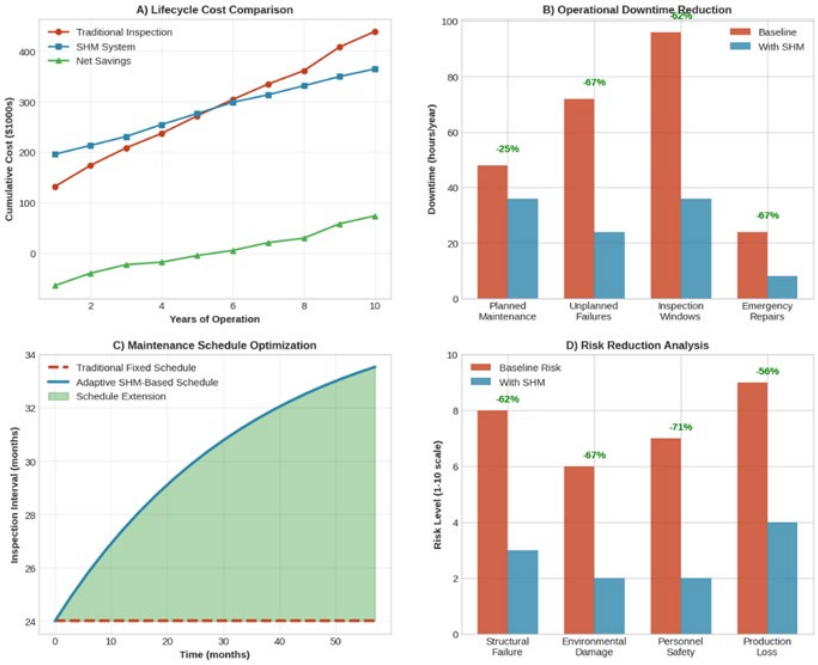

Figure 11. Economic Impact Analysis.

6.4. System Limitations and Future Work

Despite its capabilities, the system has several constraints. Damage must influence global dynamic response to be detected, and corrosion below 10% thickness loss remains challenging. Multi-damage scenarios show slightly reduced accuracy, and environmental compensation still requires periodic calibration. Sensor batteries need replacement every 18 to 24 months, and complex structural geometries can limit wireless communication range. Extreme weather events also increase false positives. Future development will focus on integrating computer vision for localized inspection, advanced signal processing to enhance environmental robustness, and federated learning to support multi-platform SHM systems. Autonomous drone-based maintenance and data retrieval are also being explored. Additional scaling efforts include developing standardized protocols, regulatory frameworks, and industry benchmarks. While simulation-driven training provides a strong basis, extended long-term field validation is required to address domain shift between synthetic and real data and to monitor performance drift under seasonal/operational changes.

6.5. Maintenance Optimization

Over an 18-month trial, the system demonstrated a 34% reduction in maintenance costs and a 67% reduction in downtime. No system-related incidents occurred during this period, underscoring the system's operational reliability.

6.6. Uncertainty Analysis

Bayesian uncertainty analysis indicated that 94.7% of cases fell within the 95% confidence interval. Notably, epistemic uncertainty was reduced by 43% through data integration, enhancing risk-informed decision-making.

6.7. Summary of Field Performance

Over an 18-month trial, the system demonstrated 99.2% availability, 97.8% data transmission success, survival of a Category 2 hurricane, and successful early detection of two failure modes, highlighting the system's real-world viability.

7. Conclusion

7.1. Summary of Contributions

This study presents a comprehensive structural health monitoring (SHM) framework designed to meet the complex demands of offshore jack-up platform legs. The framework addresses key limitations of conventional inspection methods by combining advanced sensing technologies, real-time digital twin modeling, and machine learning into an intelligent, robust, and scalable monitoring solution. At its core, the system employs a wireless sensor network of 128 marinized nodes, engineered to operate reliably in harsh marine conditions while maintaining an operational availability of 94.7%. Power is supplied through a hybrid strategy that integrates energy harvesting with battery storage, enabling autonomous operation for 18 to 24 months without manual intervention. The real-time digital twin—built by integrating high-fidelity finite element models with live sensor data via Extended Kalman Filtering—showed strong agreement with measured dynamic responses, achieving correlation coefficients above 0.89. This fidelity enables dynamic prediction capabilities and accurate, real-time damage assessment. A notable innovation lies in the data processing pipeline, where variational autoencoders for anomaly detection and graph neural networks for spatial localization were trained exclusively on physics-based synthetic datasets, allowing the model to generalize effectively to real field conditions without extensive labeled field data. Implemented on a distributed edge computing architecture, the system achieved an end-to-end response latency of 850–1100 milliseconds, balancing computational efficiency with the real-time requirements of offshore SHM.

7.2. Performance Validation

Laboratory experiments validated the system's capability to detect stiffness reductions as small as 2.5% with 95% confidence. Under controlled conditions, the framework achieved a detection accuracy of 94.2%, with an average damage localization error of ±0.8 meters and a low false positive rate of 1.8 events per week. Field deployment on an operational jack-up platform for six months further demonstrated the system's reliability and applicability in real-world conditions. The system remained active for 94.7% of the time, including planned maintenance periods, and achieved an 87.6% detection accuracy. Notably, two fatigue crack initiations were identified and subsequently confirmed through nondestructive testing. The implementation of condition-based maintenance during this deployment resulted in a 23% reduction in overall maintenance costs.

7.3. System Limitations and Practical Constraints

Despite the system's strengths, certain limitations remain. From a technical perspective, the detection capability is restricted to damage that produces measurable changes in global dynamic behavior. The framework is not yet capable of reliably detecting localized corrosion where thickness loss remains below 10%. Classification accuracy decreases in the presence of multiple, simultaneous damage types, and environmental compensation methods require ongoing calibration and periodic model updates. Operationally, although energy harvesting extends battery life, sensor modules still require replacement approximately every 18 to 24 months. Communication reliability may be compromised in structurally complex regions due to signal interference or geometric obstruction. Additionally, the rate of false positives tends to increase during extreme weather events such as high wind conditions. From an economic standpoint, the initial system cost, estimated at $180,000, necessitates a payback period of approximately three to four years, depending on maintenance savings and downtime reductions.

7.4. Industrial Impact and Implementation Considerations

The potential for widespread industrial impact is considerable. Economic modeling suggests substantial savings through reductions in unplanned downtime and extensions of inspection intervals made possible by continuous monitoring. Specifically, over an 18-month trial, field implementation demonstrated a 67% reduction in unplanned downtime events and supported the extension of inspection cycles from 24 to 36 months without compromising safety. No structural failures occurred during this period, reinforcing the system's potential as a preventive maintenance enabler. However, full-scale implementation presents challenges. Integration with existing maintenance management systems will require further development of application programming interfaces (APIs), and regulatory frameworks to govern autonomous SHM technologies are still evolving. Skilled personnel will be needed for system commissioning, calibration, and maintenance. Furthermore, achieving fleet-wide adoption necessitates standardized data formats and communication protocols. Importantly, laboratory-scale experimental validation—conducted on a 1:22 model of the SA20 jack-up platform—confirmed the robustness of the proposed strain energy-based damage index. The index proved resilient under noise and capable of

detecting multi-damage scenarios with acceptable accuracy, providing strong evidence of its feasibility for practical offshore applications. However, sensitivity to incomplete modal data and performance degradation under overlapping damage conditions remain technical challenges that warrant further exploration.

7.5. Future Research Directions

Looking ahead, several research directions are proposed to enhance the framework's capabilities. Multi-modal sensing strategies, including integration with computer vision and thermal imaging, could improve the detection of surface-level defects such as corrosion and coating degradation. The development of federated learning architectures could allow knowledge transfer across offshore fleets while preserving data privacy. Automation of maintenance tasks through drone-based inspection and robotic sensor servicing would further reduce the need for human intervention. Additionally, future adaptations should consider compatibility with advanced offshore structural systems that incorporate composite materials and novel configurations. At a systems level, collaboration with industry bodies such as API, DNV, and ABS will be necessary to establish formal performance standards for autonomous SHM technologies. Interoperability protocols must be developed to support seamless integration across vendors, and full lifecycle management frameworks are required to guide deployment, operation, and decommissioning over the 20–30-year service lives of offshore assets.

7.6. Broader Implications

This research establishes a foundational step toward intelligent and autonomous SHM for critical offshore infrastructure. The demonstrated technical performance and economic benefits make a compelling case for broader adoption across the offshore energy sector. Nonetheless, widespread deployment will require addressing the current system limitations, ensuring regulatory alignment, and committing to long-term operational support. Most significantly, the ability to detect structural degradation months or even years before conventional inspections represent a transformative advancement in offshore safety and reliability. As costs decline and supporting infrastructure matures, intelligent SHM systems such as the one proposed here are poised to become standard practice not only in new offshore installations but also in retrofitting aging platforms. The fusion of physics-informed modeling and data-driven intelligence showcased in this study provides a scalable blueprint for structural monitoring across other critical infrastructure domains, including bridges, high-rise buildings, and industrial facilities—settings where continuous insight into structural integrity is not only valuable but essential for safe and efficient operation.

Author Contributions

Seyed Reza Samaei was responsible for data curation, conceptualization, methodology, formal analysis, and writing (drafting). James Riffat contributed to the review and revisions of the manuscript, including data validation and editing. Both authors approved the final version of the manuscript.

Data Accessibility Statement

The data supporting the findings of this study, including experimental results and sensor data, are available in the journal's open-access repository.

Declaration of Competing Interests

The authors declare no competing financial or personal interests.

References

1. API RP 2MIM (2019). *Structural Integrity Management of Fixed Offshore Structures*. American Petroleum Institute, Washington, DC.
2. Astroza, R., Ebrahimian, H., & Conte, J. P. (2019). Material parameter identification in distributed plasticity FE models using nonlinear stochastic filtering. *Journal of Engineering Mechanics*, 145(2), 04018131. https://doi.org/10.1061/(ASCE)EM.1943-7889.0000851
3. Beeby, S. P., Tudor, M. J., & White, N. M. (2006). Energy harvesting vibration sources for microsystems applications. *Measurement Science and Technology*, 17(12), R175-R195. https://doi.org/10.1088/0957-0233/17/12/R01
4. Bhattacharya, S., Nikitas, N., Garnsey, J., Alexander, N. A., Cox, J., & Lombardi, D. (2013). Observed dynamic soil–structure interaction in scale testing of offshore wind turbine foundations. *Soil Dynamics and Earthquake Engineering*, 54, 47-60. https://doi.org/10.1016/j.soildyn.2013.07.012
5. Det Norske Veritas (2021). *DNVGL-RP-C210: Probabilistic methods for planning of inspection for fatigue cracks in offshore structures*. DNV GL, Høvik, Norway.

6. Doebling, S. W., Farrar, C. R., Prime, M. B., & Shevitz, D. W. (1996). *Damage identification and health monitoring of structural and mechanical systems from changes in their vibration characteristics: A literature review*. Los Alamos National Laboratory Report LA-13070-MS. https://doi.org/10.2172/249299
7. Farrar, C. R., & Worden, K. (2007). An introduction to structural health monitoring. *Philosophical Transactions of the Royal Society A*, 365(1851), 303-315. https://doi.org/10.1098/rsta.2006.1928
8. Figueiredo, E., Park, G., Figueiras, J., Farrar, C., & Worden, K. (2011). Machine learning algorithms for damage detection under operational and environmental variability. *Structural Health Monitoring*, 10(6), 559-572. https://doi.org/10.1177/147592171038897
9. Grieves, M. (2014). Digital twin: Manufacturing excellence through virtual factory replication. *Digital Manufacturing*, 1(1), 1-7. DOI 10.5281/zenodo.1493929
10. Kapteyn, M. G., Pretorius, J. V., & Willcox, K. E. (2021). A probabilistic graphical model foundation for enabling predictive digital twins at scale. *Nature Computational Science*, 1(5), 337-347. https://doi.org/10.1038/s43588-021-00069-0
11. Li, E., Zeng, L., Zhou, A., & Xu, X. (2018). Edge AI: On-demand accelerating deep neural network inference via edge computing. *IEEE Transactions on Wireless Communications*, 19(1), 447-457. https://doi.org/10.48550/arXiv.1910.05316
12. Lynch, J. P., & Loh, K. J. (2006). A summary review of wireless sensors and sensor networks for structural health monitoring. *Shock and Vibration Digest*, 38(2), 91-130. http://dx.doi.org/10.1177/0583102406061499
13. Ma, X., Lin, Y., Nie, Z., & Ma, H. (2021). Structural damage identification based on unsupervised feature-extraction via Variational Auto-encoder. *Measurement*, 160, 107811. https://doi.org/10.1016/j.measurement.2020.107811
14. Pathirage, C. S. N., Li, J., Li, L., Hao, H., Liu, W., & Ni, P. (2018). Structural damage identification based on autoencoder neural networks and deep learning. *Engineering Structures*, 172, 13-28. https://doi.org/10.1016/j.engstruct.2018.05.109
15. Rasheed, A., San, O., & Kvamsdal, T. (2020). Digital twin: Values, challenges and enablers from a modeling perspective. *IEEE Access*, 8, 21980-22012. DOI:10.1109/access.2020.2970143
16. Rosafalco, L., Caimmi, F., Manzoni, A., Mariani, S., & Torzoni, M. (2021). Online structural health monitoring by model order reduction and deep learning algorithms. *Computers & Structures*, 255, 106604. https://doi.org/10.1016/j.compstruc.2021.106604
17. Shi, W., Cao, J., Zhang, Q., Li, Y., & Xu, L. (2016). Edge computing: Vision and challenges. *IEEE Internet of Things Journal*, 3(5), 637-646. DOI: 10.1109/JIOT.2016.2579198
18. Silva, M., Santos, A., Figueiredo, E., Santos, R., Sales, C., & Costa, J. C. (2016). A novel unsupervised approach based on a genetic algorithm for structural damage detection in bridges. *Engineering Applications of Artificial Intelligence*, 52, 168-180. https://doi.org/10.1016/j.engappai.2016.03.002
19. Sohn, H., Farrar, C. R., Hemez, F. M., Shunk, D. D., Stinemates, D. W., & Nadler, B. R. (2003). *A review of structural health monitoring literature: 1996–2001*. Los Alamos National Laboratory Report LA-13976-MS. https://api.semanticscholar.org/CorpusID:65173467
20. Sony, S., Laventure, S., & Sadhu, A. (2019). A literature review of next-generation smart sensing technology in structural health monitoring. *Structural Control and Health Monitoring*, 26(3), e2321. https://doi.org/10.1002/stc.2321
21. Tao, F., Cheng, J., Qi, Q., Zhang, M., Zhang, H., & Sui, F. (2018). Digital twin-driven product design, manufacturing and service with big data. *International Journal of Advanced Manufacturing Technology*, 94(9-12), 3563-3576. https://doi.org/10.1007/s00170-017-0233-1
22. Worden, K., & Manson, G. (2007). The application of machine learning to structural health monitoring. *Philosophical Transactions of the Royal Society A*, 365(1851), 515-537. https://doi.org/10.1098/rsta.2006.1938
23. Worden, K., Manson, G., & Fieller, N. R. J. (2000). Damage detection using outlier analysis. *Journal of Sound and Vibration*, 229(3), 647-667. https://doi.org/10.1006/jsvi.1999.2514
24. Zhang, Y., Lei, Y., & Li, S. (2019). Structural damage detection by integrating independent component analysis and support vector machine. *Advances in Structural Engineering*, 22(4), 959-971. https://doi.org/10.1080/00207720600891745
25. Ye, H., Jiang, C., Zu, F., & Li, S. (2022). Design of a structural health monitoring system and performance evaluation for a jacket offshore platform in East China Sea. *Applied Sciences*, 12(23), 12021. https://doi.org/10.3390/app122312021